Accuracy-Complexity Tradeoff Analysis and Complexity Reduction Methods for Non-Stationary IMT-A MIMO Channel Models

YAN ZHANG[1], (Member, IEEE), AMMAR GHAZAL[2], (Member, IEEE), CHENG-XIANG WANG[3,4], (Fellow, IEEE), HONGRUI ZHOU[5], WEIMING DUAN[5], AND EL-HADI M.AGGOUNE[6], (Senior Member, IEEE)

[1]School of Information and Electronics, Beijing Institute of Technology, Beijing, 100081, China
[2]Institute of Engineering Sciences, Faculty of Computing Engineering and Media, De Montfort University, LE1 9BH, U. K.
[3]National Mobile Communications Research Laboratory, School of Information Science and Engineering, Southeast University, Nanjing 210096, China [4]Purple Mountain Laboratories, Nanjing 211111, China
[5]Shanghai Research Institute, Huawei Technologies Co., Ltd., Shanghai, 201206, China
[6]Sensor Networks and Cellular Systems Research Center, University of Tabuk, Tabuk, 47315/4031, Saudi Arabia

Corresponding author: Cheng-Xiang Wang (chxwang@seu.edu.cn).

This work was supported in part by the National Key R&D Program of China under Grant 2018YFB1801101, in part by the Natural Science Foundation of China (NSFC) under Grant 61960206006 and 61871035, in part by the Fundamental Research Funds for the Central Universities under Grant 2242019R30001, in part by the EU H2020 RISE TESTBED Project under Grant 734325, in part by the National High Technology Research and Development Program of China under Grant 2015AA01A706, and in part by the Sensor Networks and Cellular Systems (SNCS) Research Center, University of Tabuk.

ABSTRACT High-mobility wireless communication systems have attracted growing interests in recent years. For the deployment of these systems, one fundamental work is to build accurate and efficient channel models. In high-mobility scenarios, it has been shown that the standardized channel models, e.g., IMT-Advanced (IMT-A) multiple-input multiple-output (MIMO) channel model, provide noticeable longer stationary intervals than measured results and the wide-sense stationary (WSS) assumption may be violated. Thus, the non-stationarity should be introduced to the IMT-A MIMO channel model to mimic the channel characteristics more accurately without losing too much efficiency. In this paper, we analyze and compare the computational complexity of the original WSS and non-stationary IMT-A MIMO channel models. Both the number of real operations and simulation time are used as complexity metrics. Since introducing the non-stationarity to the IMT-A MIMO channel model causes extra computational complexity, some computation reduction methods are proposed to simplify the non-stationary IMT-A MIMO channel model while retaining an acceptable accuracy. Statistical properties including the temporal autocorrelation function, spatial cross-correlation function, and stationary interval are chosen as the accuracy metrics for verifications. It is shown that the tradeoff between the computational complexity and modeling accuracy can be achieved by using these proposed complexity reduction methods.

INDEX TERMS IMT-A MIMO channel model, non-stationary IMT-A MIMO channel model, model complexity analysis, statistical properties, complexity reduction methods.

Nomenclature

$(\cdot)^*$	Complex conjugation operation.
λ	Wavelength.
$\lfloor\cdot\rfloor$	Floor function.
$\max(\cdot)$	Maximum.
ρ	Polarization.
τ_n	Normalized delay of the n-th ($n = 1, \cdots, N$) cluster.
$\mathrm{E}\{\cdot\}$	Statistical expectation operator.
$a(t)$	Distance between the last bounce/scatterer and mobile station (MS) at time t.
$c(t)$	Distance between base station (BS) and the first bounce/scatterer at time t.
L	Mean value of the number of newly generated clus-

ters.

M	Number of rays within each cluster.
N	Number of clusters.
P_n	Power of the n-th cluster.
S	Number of transmitter (Tx) antenna elements.
s_{ASA}	Log-normal distributed random variable (RV) of angle spread of arrival (ASA).
s_{ASD}	Log-normal distributed RV of angle spread of departure (ASD).
s_{DS}	Log-normal distributed RV of delay spread (DS).
s_{SF}	Log-normal distributed RV of shadow fading (SF).
s_K	Log-normal distributed RV of Rician K-factor.
T	The number of time samples.
U	Number of receiver (Rx) antenna elements.
v, θ_v	Speed and mobile direction of MS, respectively.
v_c, θ_c	Speed and mobile direction of mobile scatterer, respectively.
$\phi_{n,m}$	Angle of departure (AoD) related to the m-th ($m = 1, \cdots, M$) ray within the n-th cluster.
$\Phi_{m,n}$	Random initial phases related to the m-th ray within the n-th cluster.
$\upsilon_{n,m}$	Doppler frequency component related to the m-th ray within the n-th cluster.
$\varphi_{n,m}$	Angle of arrival (AoA) related to the m-th ray within the n-th cluster.

I. INTRODUCTION

THE deployments of wireless communication systems in trains or vehicles have become more popular in recent years. They aim at providing continuous wireless access services even in high-mobility scenarios. To design and explore the wireless communication systems in high-speed trains (HSTs) or vehicle-to-vehicle (V2V) applications, it is fundamental to investigate the underlying propagation channel characteristics and to develop accurate and efficient models to mimic the realistic wireless channels.

Most of the existing standardized channel models assume that channels satisfy the wide-sense stationary (WSS) assumption. However, measurement results [1]–[9] have proved that the measured stationary intervals, defined as the maximum time over which the WSS assumption is valid, for high-mobility scenarios are much shorter than those of standardized channel models. Therefore, it is crucial to take non-stationarity into account in developing channel models for high-mobility scenarios [10]–[17]. As an example, in [18] we proposed a non-stationary IMT-A multiple-input multiple-output (MIMO) channel model to investigate the time evolution of wireless channels in high-mobility scenarios by considering small-scale time-variant parameters. Supported by a comprehensive analysis of the simulation results, it was demonstrated that the proposed non-stationary IMT-A MIMO channel model can accurately mimic the characteristics of high-mobility channels [18].

Realistic channel models should be sufficiently accurate in modeling the underlying channel characteristics while retaining an acceptable computational complexity of generating the channel coefficients. Therefore, two criteria including the modeling accuracy and the efficiency should be both considered in evaluating the performance of any developed channel models. In general, introducing the non-stationarity will increase the complexity of the channel model, which are crucial for system-level simulation or other applications. However, the computational complexity brought by the non-stationarity has not been discussed in existing research work.

In the literature, the complexities of some channel models have been investigated. In [19], the complexities of correlation-based and geometric-based stochastic MIMO channel modeling methods were compared. It was shown that when the numbers of antenna elements increase to 4×4 MIMO or higher, the geometric method requires less descriptive parameters than correlation-based method [19]. In [20], the computational complexities of drop-based radio channel simulation were calculated based on the WINNER II channel model. However, to the best of our knowledge, the computational complexities of the standardized IMT-A MIMO channel model have not been well-quantized and thoroughly investigated.

To reflect real channels as accurately as possible, channel models become very complicated, especially with a large system bandwidth and a large number of antenna elements [21]. With multiple links and numerous drops, using complicated channel models for the system-level simulations would require large time consumption and computation resources. Thus, the accuracy-complexity tradeoff must be considered in the modeling procedure. Recently, some complexity reduction methods were proposed to ensure the implementation efficiency of channel models. Thus, some complexity reduction methods were proposed to ensure the implementation efficiency of the channel models. In [22], an alternative implementation called non-uniform scattering cross section was proposed to efficiently implement the GBSM. In [23], three different levels of modeling complexity were defined in order to limit the computational effort for the extensive simulations of a stochastic radio channel model. In [24], a low-complexity algorithm exploiting the low-dimensional subspace spanned by multidimensional prolate spheroidal sequences was presented for the computer simulation of GBSMs. A similar approach was also used in [25] to overcome the complexity constraint in the geometry-based modeling of diffuse components. In [26], the IMT-A MIMO channel model was extended to a device-to-device (D2D) channel and the Doppler response-based fast fading channel generation was proposed to reduce the simulation time. Several potential simplifications of the GBSMs to reduce the complexity with minimal impact on accuracy were investigated in [27]. For urban micro-cellular scenarios, the authors in [28] proposed an improved IMT-A GBSM which can reduce the complexity without losing much accuracy. In [29], a vehicular channel emulator based on field-programmable gate array (FPGA) is implemented for real-time performance evaluation of IEEE 802.11p transceivers.

The introduction of the non-stationarity to the channel

model causes extra complexity due to the periodic update of time-variant parameters. A cluster-based non-stationary vehicular channel model was developed with low computational complexity in [30]. A complexity reduction method aiming at determining the minimum number of the relevant clusters was applied to the real-time emulation of non-stationary channels in [31]. A compact channel emulation scheme with low complexity on a FPGA platform was developed and validated in [32]. In [33] and [34], real time channel emulation methods and signal processing algorithms were introduced for non-stationary vehicular scenarios based on geometry-based stochastic channel models. The non-stationary fading process was partitioned into a sequence of local stationarity regions and a subspace projection of the propagation path parameters was adopted to compress the time-variant channel impulse response.

Quantizing the complexity of channel models is useful for the fast system-level simulations and real-time implementation of emulators. On basis of this work, the time-consuming steps can be found and then the computational complexity can be reduced. In [18], the accuracy of the non-stationary IMT-A MIMO channel model has been verified but the complexity has not been assessed. For practical applications of the non-stationary IMT-A MIMO channel model, the resulting increase of the computational complexity should be evaluated and methods to reduce this complexity need to be provided.

Reflecting on the aforementioned research gaps, in this paper we analyze the complexity of the original WSS IMT-A MIMO channel model by using the number of real operations (ROs) and simulation time as metrics. Based on our previous work [18], the complexity of the developed non-stationary IMT-A MIMO channel model is compared with that of the original WSS IMT-A MIMO channel model. Furthermore, some complexity reduction methods are proposed to improve the efficiency of the non-stationary IMT-A MIMO channel model for system-level simulations.

The novelty and main contributions of this paper are summarized as follows.

(1) We derive and compare the computational complexities of the original WSS and non-stationary IMT-A MIMO channel models. Two metrics, i.e., the number of ROs and simulation time, are used to quantize the complexity of the channel models. The impacts of introducing non-stationarity into the IMT-A MIMO channel model on its computational complexity are thoroughly evaluated.

(2) To simplify the non-stationary IMT-A MIMO channel model, two complexity reduction methods are proposed to offer a better tradeoff between the model accuracy and complexity. The proposed methods are useful to improve the efficiency of non-stationary IMT-A MIMO channel models and can provide guidance for the simplification of other non-stationary channel models.

(3)We further analyze the tradeoff between the accuracy and complexity of various simplified n on-stationary IMT-A MIMO channel models by adjusting different channel model parameters.

In this study, the complexity of the original and non-stationary IMT-A MIMO channel models are qualified. The impacts of the introduction of non-stationarity on the computational complexity of channel models are evaluated. The proposed complexity reduction methods can be used to improve the efficiency of the non-stationary IMT-A MIMO channel model and to provide references to applications of other non-stationary channel models.

The remainder of this paper is organized as follows. The computational complexities of the original WSS and non-stationary IMT-A MIMO channel models are analyzed in Section II and Section III, respectively. The comparison results are shown in Section IV. The complexity reduction methods are proposed in Section V. Finally, the conclusions are drawn in Section V.

II. COMPUTATIONAL COMPLEXITY ANALYSIS OF THE ORIGINAL WSS IMT-A MIMO CHANNEL MODEL

In this section, we analyze the complexity of generating time-variant MIMO channel coefficients in the original WSS IMT-A MIMO channel model in terms of the required number of ROs, following the coefficients generation procedure detailed in [35]. The analysis of computational complexity is in terms of the number of real operations (ROs) introduced in [19] and [20]. The number of ROs of any mathematical operations is calculated based on four basic operations, namely real addition, real multiplication, real division, and table lookup, with each operation requiring one RO [19]. Table lookup is to find values in a precalculated and stored table with a simple array indexing operation, which can save significant processing time. Complex number and other mathematical operations are transformed into or approximated by these four basic operations. For example, complex multiplication is corresponding to the multiplication between two complex numbers, which requires 6 ROs (4 real multiplications and 2 real addition). It should be noted that multiplying a real number x by the imaginary unit j, i.e., jx, does not need any RO because no result is calculated. Similarly, the complex division requires 11 ROs and the complex addition needs 2 ROs. Table 1 illustrates the required number of ROs for several mathematical operations.

Please note that in the following analysis, only the processing required for generating time-variant samples for a single link is considered. All the pre-processing like correlation matrix factorization or lookup table generation is excluded from the examination. If a system-level simulation is considered, i.e., there are $K(K > 1)$ links in the system, then the total number of ROs should be obtained by multiplying K by the reported RO numbers per link. The path loss (PL), which determines the signal-to-noise ratio (SNR), is described by different models according to the scenarios and line-of-sight (LoS) conditions, as summarized in Table A1-2 in [35]. The number of ROs for calculating the path loss is between 6 and 29, which is the same for both the original and the non-stationary IMT-A MIMO channel models. Then, it is

TABLE 1. Required number of ROs for typical mathematical operations [19].

Operation	Required number of ROs
Exponential (e^x)	15
Uniform distributed RV	5
Gaussian distributed RV	72
Complex Multiplication	6
Complex Division	11
Complex Addition	2
Complex Norm	5
Sin(x)	7
Cos(x)	8
Table lookup	8
Log(x)	1
Real square root	1

excluded from the complexity comparison, as in [19] and [20]. The number of ROs required for single-link channel coefficient generation in the original WSS IMT-A MIMO channel model is clarified as follows.

A. GENERATION OF CORRELATED LARGE SCALE PARAMETERS (LSPS)

In the original WSS IMT-A MIMO channel model, there are five LSPs, including DS, ASA, ASD, SF, and Rician K-factor. All these LSPs follow log-normal distributions and they can be generated following the procedure described in [36].

First, the cross-correlation between these $Z = 5$ LSPs is generated independently to the LSPs by a linear transformation, i.e.,

$$\tilde{s}_{Z\times 1} = \sqrt{C_{Z\times Z}}\xi_{Z\times 1} \tag{1}$$

where $C_{Z\times Z}$ is the correlation matrix as defined in [35]. Correlation matrix factorization is excluded from the complexity analysis because the matrix will not vary from link to link and the factorization can be pre-processed. Note that $\xi_{Z\times 1}$ is a vector of Z independent zero-mean Gaussian RVs, while $\tilde{s}_{Z\times 1} = [\tilde{s}_{\text{DS}}, \tilde{s}_{\text{ASA}}, \tilde{s}_{\text{ASD}}, \tilde{s}_{\text{SF}}, \tilde{s}_K]^T$. From Table 1, generating a Gaussian RV requires 72 ROs. Therefore, $72 \times 5 = 360$ ROs are required to generate the vector $\xi_{Z\times 1}$. The multiplication of a matrix of the square roots of the 5×5 correlation matrix by a 5×1 vector requires 5×5 real multiplications and 5×4 real additions. As a result, the required number of ROs is

$$C_{\text{LS\_corr}} = (72 + 5 + 4) \times 5 = 405. \tag{2}$$

Then, we need to transform the elements of $\xi_{Z\times 1}$ into log-normal distributed RVs. The log-normal distributed RV of the DS is given by

$$s_{\text{DS}} = 10^{(\sigma_{\text{DS}}\tilde{s}_{\text{DS}}+\mu_{\text{DS}})} \tag{3}$$

where μ_{DS} is the logarithmic mean of the distribution of DS and σ_{DS} is the logarithmic standard deviation of the distribution of DS. Similarly, the log-normal distributed RV of the ASA/ASD is given by

$$s_{\text{ASA/ASD}} = 10^{(\sigma_{\text{ASA/ASD}}\tilde{s}_{\text{ASA/ASD}}+\mu_{\text{ASA/ASD}})} \tag{4}$$

where $\mu_{\text{ASA/ASD}}$ is the logarithmic mean of the distribution of ASA/ASD and $\sigma_{\text{ASA/ASD}}$ is the logarithmic standard deviation of the distribution of ASA/ASD. The log-normal distributed RV of the SF is given by

$$s_{\text{SF}} = 10^{(\sigma_{\text{SF}}\tilde{s}_{\text{SF}}/10)} \tag{5}$$

where σ_{SF} is the logarithmic standard deviation of the distribution of SF. Finally, the log-normal distributed RV of K-factor is given by

$$s_K = 10^{(\sigma_K\tilde{s}_K+\mu_K/10)} \tag{6}$$

where μ_K is the logarithmic mean of the distribution of SF and σ_K is the logarithmic standard deviation of the distribution of K-factor.

Note that calculating $10^x = e^{x\ln 10}$ needs 17 ROs (15 for calculating the exponential, 1 for multiplexing, and 1 for logarithm). Then, 2 ROs are needed to calculate x for s_{DS} and $s_{\text{ASA/ASD}}$, and 3 ROs for s_K. For s_{SF}, calculating x requires 2 ROs (division and multiplication). Thus, transforming elements of $\xi_{Z\times 1}$ into 5 log-normal distributed RVs requires

$$C_{\text{trans}} = 5 \times 17 + 3\times 2 + 2 + 3 = 96. \tag{7}$$

The total number of the ROs required to generate the correlated LSPs in the original WSS IMT-A MIMO channel model is

$$C_{\text{LS}} = C_{\text{LS\_corr}} + C_{\text{trans}} = 501. \tag{8}$$

B. GENERATION OF SMALL SCALE PARAMETERS (SSPS)

1) Generate Delays

The delay of the n-th cluster follows an exponential distribution and it can be expressed as

$$\tau_n{}' = -r_\tau\sigma_\tau \ln(X_n) \tag{9}$$

where r_τ is the delay distribution factor, σ_τ is the DS, and X_n is a uniform distributed RV. Calculations of (9) require 1 logarithm and 2 real multiplications, in addition to 5 ROs to generate the uniform distributed RV X_n. The delays $\tau_n{}'$ can be subtracted by the smallest one and then sorted in a descending order to get normalized delays τ_n. The normalization process costs 1 RO for each delay, while the descending order costs $(N-1)^2$ ROs. Thus, the number of ROs required to generate the delays is

$$C_\tau = (2 + 1 + 5 + 1)N + (N-1)^2 = N^2 + 7N + 1. \tag{10}$$

2) Generate Cluster Powers

The cluster powers are calculated by

$$P_n = \exp\left(-\tau_n\frac{r_\tau - 1}{r_\tau\sigma_\tau}\right)10^{-\frac{Z_n}{10}} \tag{11}$$

where Z_n is a Gaussian RV representing the per cluster shadowing term. Calculating the left exponential costs 4 ROs (2 multiplications, 1 division, and 1 subtraction) and 15 ROs for the exponential function. 1 RO (multiplication) is required to multiply the left term and the right term.

Calculating the expression $10^{-\frac{Z_n}{10}}$ costs 1 real division, 17 ROs for 10^x, and 72 ROs to generate the Gaussian RV Z_n. The power will be normalized so that the sum of all cluster powers is equal to one. This normalization process costs $N-1$ real additions and N real divisions. Therefore, the number of ROs to generate the cluster powers is

$$C_{\text{P}} = (4+15)+(17+1+72)+1+N+(N-1) = 2N+109. \tag{12}$$

3) Generate AoAs and AoDs

In the original WSS IMT-A MIMO channel model, the power azimuth spectrum (PASs) are modeled as the following wrapped Gaussian distributions for all the scenarios except for the indoor hot spot (InH) one

$$\varphi_n{}' = \frac{2\sigma_{\text{AoA}}\sqrt{-\ln\left(\frac{P_n}{\max P_n}\right)}}{C}. \tag{13}$$

For the InH scenario, the PAS is modeled as the following Laplacian distribution

$$\varphi_n{}' = \frac{2\sigma_{\varphi}\sqrt{-\ln\left(\frac{P_n}{\max P_n}\right)}}{C} \tag{14}$$

where C is a tabulated scaling factor and $\sigma_{\text{AoA}} = \sigma_{\varphi}/1.4$ is the standard deviation of the AoA. The maximum operation needs $N-1$ ROs, which only needs to be carried out once for all clusters. In both cases, calculating $\varphi_n{}'$ costs 2 real divisions, 1 logarithm, 1 square root, and 2 real multiplications, totaling 6 ROs per cluster.

To introduce random variation, we have

$$\varphi_n = X_n\varphi_n{}' + Y_n + \varphi_{\text{LoS}} \tag{15}$$

where X_n is a uniform distributed RV within the discrete set of {1, -1}, Y_n is a Gaussian distributed RV, and φ_{LoS} is the LoS direction defined in the network layout. From Table 1, X_n needs 5 ROs and Y_n needs 72 ROs. In (15), 1 multiplication and 2 additions are also required. Thus, to generate φ_n, we need $(5+72+1+2) = 80$ ROs per cluster.

The AoA of the m-th ray of the n-th cluster is calculated by using

$$\varphi_{n,m} = \varphi_n + c_{\text{AoA}}\alpha_m \tag{16}$$

where c_{AoA} is the tabulated cluster azimuth spread of arrival angles and α_m is the tabulated offset angle. Only 2 ROs (1 multiplication and 1 addition) are needed for each ray. Therefore, the required number of ROs is

$$C_{\text{az}} = (N-1)+2\left((6+80)N+2NM\right) = 173N+4MN-1. \tag{17}$$

4) Random Coupling of Rays within Clusters

The random coupling of AoDs $\phi_{n,m}$ to AoAs $\varphi_{n,m}$ can be realized by assigning a RV with a uniform distribution to the M rays within a cluster n, or within a sub-cluster in case of two strongest clusters. Thus, the required number of ROs is

$$C_{\text{coup}} = 5MN. \tag{18}$$

Finally, from (10), (12), (17), and (18), the total number of ROs to generate SSPs is

$$\begin{aligned} C_{\text{SS}} &= C_{\tau} + C_{\text{P}} + C_{\text{az}} + C_{\text{coup}} \\ &= N^2 + 182N + 9MN + 109. \end{aligned} \tag{19}$$

C. GENERATION OF INITIAL CHANNEL COEFFICIENTS

The required number of ROs for generating the initial (first) channel coefficients in the original WSS IMT-A MIMO channel model can be calculated as

$$C_{\text{cc}} = C_{\Phi} + C_{\text{FP}} + C_{\text{H}} \tag{20}$$

where C_{Φ}, C_{FP}, and C_{H} represent the required numbers of ROs for random initial phases $\Phi_{m,n}$, field pattern (FP), and channel coefficient matrix $\mathbf{H}$, respectively.

1) Draw Random Initial Phases and Field Patterns

For each ray m of each cluster n and for four different polarization combinations, random initial phases $\left\{\Phi_{n,m}^{\text{VV}}, \Phi_{n,m}^{\text{VH}}, \Phi_{n,m}^{\text{HV}}, \Phi_{n,m}^{\text{HH}}\right\}$ need to be drawn. The initial phases have a uniform distribution within $[-\pi, \pi)$. According to Table 1, the generation of uniform distributed RVs costs 5 ROs. Thus, we can get

$$C_{\Phi} = 5\rho^2 MN. \tag{21}$$

Here, ρ is related to polarization, i.e., $\rho = 2$ in case of dual polarization and $\rho = 1$ in case of single polarization.

The measured FPs could have different representations and therefore interpolation complexities as well. Usually, we can use linear interpolation of complex samples taken with pre-defined resolution (typically 1°) [20]. Its computational complexity, per polarization, will be determined with two real subtractions, one real division, two complex additions, and one multiplication between a real number and a complex number, totaling $2+1+2\times 2+2\times 1 = 9$ ROs. Then, the complexity of generating the field pattern can be written as

$$C_{\text{FP}} = 9\left(U+S\right)\rho MN. \tag{22}$$

2) Generate Channel Coefficients for Each Cluster n and Each Rx and Tx Element Pair u, s

For the $N-2$ weakest clusters and uniform linear arrays (ULAs), the channel coefficients are given by [35]

$$h_{u,s,n}(t) = \sqrt{P_n}\times \sum_{m=1}^{M}\left\{\begin{array}{c} \begin{bmatrix} F_{\text{R}x,u,V}(\varphi_{n,m}) \\ F_{\text{R}xu,H}(\varphi_{n,m}) \end{bmatrix}^T \mathbf{A}_{n,m} \begin{bmatrix} F_{\text{T}x,s,V}(\phi_{n,m}) \\ F_{\text{T}x,s,H}(\phi_{n,m}) \end{bmatrix} \\ \exp\left[j2\pi\lambda^{-1}\left(d_s\sin(\phi_{n,m}) + d_u\sin(\varphi_{n,m})\right)\right] \\ \exp\left[j2\pi\upsilon_{n,m}t\right] \end{array}\right\}. \tag{23}$$

Here, $\mathbf{A}_{n,m}$ is used to represent the polarization matrix. In case of dual polarization,

$$\mathbf{A}_{n,m} = \begin{bmatrix} \exp\left(j\Phi_{n,m}^{\text{VV}}\right) & \sqrt{\kappa^{-1}}\exp\left(j\Phi_{n,m}^{\text{VH}}\right) \\ \sqrt{\kappa^{-1}}\exp\left(j\Phi_{n,m}^{\text{HV}}\right) & \exp\left(j\Phi_{n,m}^{\text{HH}}\right) \end{bmatrix} \tag{24}$$

which requires 4 exponentials, 1 square root, 1 real division, and 2 real multiplications. It should be noted that κ is the cross polarization ratio (XPR) which is determined by the scenario [35]. Thus, the required number of ROs to calculate $\mathbf{A}_{n,m}$ is $4\times15+1+1+2\times2=66$ ROs. Then, calculating the first row (multiplication between the three matrices) in (23) needs 6 complex multiplications and 3 complex additions, which requires $6\times6+3\times2=42$ ROs.

If ρ = 1, the polarization matrix $\mathbf{A}_{n,m}$ is reduced to $\exp(j\Phi_{n,m})$, which requires 15 ROs to obtain the exponential. Then, the first row in (23) will be reduced to $[F_{\mathrm{Rx},u}(\varphi_{n,m})]^T[\exp(j\Phi_{n,m})]\,[F_{\mathrm{Tx},s}(\phi_{n,m})]$, which requires 2 complex multiplications, i.e., 2 × 6 = 12 ROs.

The second row in the curly brackets of (23) requires 2 sines, 4 real multiplications, 1 real division, 1 real addition, and 1 exponential, i.e., $2\times7+4+1+1+15=35$ ROs.

The third row in the curly brackets of (23) is $\exp[j2\pi\upsilon_{n,m}t]$ where $\upsilon_{n,m}$ is the Doppler frequency component of ray n,m and given by

$$\upsilon_{n,m}=\lambda^{-1}v\cos(\varphi_{n,m}-\theta_v). \tag{25}$$

Thus, it requires 1 real subtraction, 1 cosine, 3 real multiplications, 1 real division, and 1 exponential, i.e., $1+8+3+1+15=28$ ROs per ray per cluster.

To multiply the first, second, and third rows together in (23), we need two complex multiplications need 6 × 2 = 12 ROs per ray per cluster. To sum up the channel coefficients of M rays, $M-1$ complex additions are required, corresponding to $2(M-1)$ ROs per cluster.

Thus, for the $N-2$ weakest clusters, the number of ROs to produce their channel coefficients is

$$C_{\text{H\_weak}}=(N-2)\,US\times((66+42+35+28+12)\,M+2\,(M-1)),\ \text{if}\ \rho=2; \tag{26a}$$

$$C_{\text{H\_weak}}=(N-2)\,US\times((15+12+35+28+12)\,M+2\,(M-1)),\ \text{if}\ \rho=1. \tag{26b}$$

For the two strongest clusters, there are three sub-clusters with fixed delay offsets {0, 5, 10 ns} in each cluster. Twenty rays of a cluster are mapped to these sub-clusters. Rays with different delay offsets are not added together. So, 2 real additions are reduced. Thus, when computing the sum of rays, the number of ROs to generate the channel coefficients of the two strongest clusters is

$$C_{\text{H\_strong}}=2US\times((66+42+35+28+12)\,M+2\,(M-3)),\ \text{if}\ \rho=2; \tag{27a}$$

$$C_{\text{H\_strong}}=2US\times((15+12+35+28+12)\,M+2\,(M-3)),\ \text{if}\ \rho=1. \tag{27b}$$

The total number of ROs required for generating the channel coefficient matrix is

$$C_{\text{H}}=C_{\text{H\_weak}}+C_{\text{H\_strong}}=(185M-2)\,USN-8US,\quad \text{if}\ \rho=2; \tag{28a}$$

$$C_{\text{H}}=C_{\text{H\_weak}}+C_{\text{H\_strong}}=(104M-2)\,USN-8US,\quad \text{if}\ \rho=1. \tag{28b}$$

Then, (20) can be calculated as

$$C_{\text{cc}}=(185M-2)\,USN-8US+18\,(U+S)\,MN+20MN,\quad \text{if}\ \rho=2; \tag{29a}$$

$$C_{\text{cc}}=(104M-2)\,USN-8US+9\,(U+S)\,MN+5MN,\quad \text{if}\ \rho=1. \tag{29b}$$

Therefore, the computational complexity to generate the initial (first) channel response in terms of the number of ROs is

$$C_{\text{initial}}=C_{\text{LS}}+C_{\text{SS}}+C_{\text{cc}}. \tag{30}$$

In case of dual polarization or single polarization,

$$C_{\text{initial}}=501+N^2+182N+29MN+109+(185M-2)USN-8US+18(U+S)MN,\quad \text{if}\ \rho=2; \tag{31a}$$

$$C_{\text{initial}}=501+N^2+182N+14MN+109+(104M-2)USN-8US+9(U+S)MN,\quad \text{if}\ \rho=1. \tag{31b}$$

D. GENERATION OF WSS CHANNEL COEFFICIENTS FOR MULTIPLE TIME SAMPLES

The operations for generating the initial channel coefficients are only implemented once, and the channel parameters including the cluster number, the powers, delays, AoAs and AoDs of clusters will not change with time in the original WSS IMT-A MIMO channel model. With time evolution, only the third row of (23) needs to be updated, which corresponds to 26 ROs per time sample. Besides, one complex multiplication with 6 ROs is needed to multiply the third row to the other parts. To sum up the channel coefficients of different rays in (23), $2(N-2)(M-1)US$ ROs are required for the $N-2$ weakest clusters, while $4(M-3)US$ ROs are needed for the two strongest clusters. Thus, the additional number of ROs required for each time sample updating is

$$C_{\text{WSS\_t}}=USNM\,(28+6)+2\,(N-2)\,(M-1)\,US+4\,(M-3)\,US=36USNM-2USN-8US. \tag{32}$$

If we need to generate channel responses for T different time samples, the total complexity of the original WSS IMT-A MIMO channel model is

$$C_{\text{WSS}}=C_{\text{initial}}+(T-1)\,C_{\text{WSS\_t}}. \tag{33}$$

III. COMPUTATIONAL COMPLEXITY ANALYSIS OF THE NON-STATIONARY IMT-A MIMO CHANNEL MODEL

Generating the channel response for the first time instance also needs C_{initial} ROs for the non-stationary IMT-A MIMO channel model. In the original WSS IMT-A MIMO channel model, only the third row in (23), $\exp[j2\pi v_{n,m}t]$ needs to be updated for each time sample. The non-stationary IMT-MIMO channel model [18] was proposed to investigate the time variation of wireless channels in high mobility scenarios. We considered small scale time-varying parameters such as the number of clusters, delays and the powers of clusters, AoDs, and AoAs. The number of clusters was described by a Markov birth-death (B-D) process. Delays, AoDs, and AoAs of clusters changed according to the geometric relationship between BS, MS, and clusters. The cluster powers were calculated assuming a single slope exponential power delay profile. Therefore, cluster number, powers, delays, and angles of clusters are all time-variant and need to be regenerated. In this section, we will analyze the computational complexity of the non-stationary IMT-A MIMO channel model.

A. UPDATE THE TIME-VARIANT CLUSTER NUMBER

In the non-stationary channels, because of the movement of the MS and/or the surrounding scatterers, the number of clusters is time-variant. The instantaneous number of clusters can be calculated based on the B-D process [37]. Here, we classify the clusters into two kinds: newly generated clusters and survived (remained) clusters. The complexity of computing the cluster number is analyzed as follows.

1) Survived Clusters at Time Instance t

Observing a time series of channel impulse responses (CIRs), each cluster remains at time instance $t = t_{k+1}$ with the probability

$$P_r\left(\delta_{P,k}\left(t\right)\right) = e^{-\lambda_R \delta_{P,k}(t)}. \tag{34}$$

where λ_R is the recombination rate [37]. The channel fluctuation $\delta_{P,k}\left(t\right)$ is a means of measuring the changes taking place in the scattering environments and it can be defined as

$$\delta_{P,k}\left(t\right) = \delta_{\text{MC},k}\left(t\right) + \delta_{\text{MS},k}\left(t\right) \tag{35}$$

where $\delta_{\text{MC},k}\left(t\right)$ and $\delta_{\text{MS},k}\left(t\right)$ denote the fluctuations caused by the scatterer and MS movement, respectively.

$$\delta_{\text{MC},k}\left(t\right) = P_c v_c \left(t_{k+1} - t_k\right) \tag{36}$$

and

$$\delta_{\text{MS},k}\left(t\right) = v\left(t_{k+1} - t_k\right) \tag{37}$$

where P_c is the percentage of moving scatterers and t_k is the time of the k-th time sample (instance).

To judge which cluster can survive at the next time instance $t = t_{k+1}$, we need to generate $N_{\text{total}}\left(t_k\right)$ uniform distributed RVs within $[0, 1]$, requiring 5 ROs per cluster. $N_{\text{total}}\left(t_k\right)$ is the total cluster number at $t = t_{k+1}$. After comparing $P_r\left(t\right)$ with these RVs, we can decide whether a cluster remains or not. Thus, the total complexity to get the number of the survived clusters is

$$C_{\text{SurNum}}\left(t\right) = \left(5+1\right) N_{\text{total}}\left(t_k\right). \tag{38}$$

In [18], the expectation of the total cluster number, also defined as the initial number, is given by

$$\text{E}\{N_{\text{total}}\left(t_k\right)\} = N\left(t_0\right) = \frac{\lambda_G}{\lambda_R} = N. \tag{39}$$

Here, λ_G is the generation rate [37]. Thus, the mean number of ROs to compute the survived cluster number is

$$C_{\text{SurNum}} = 6N. \tag{40}$$

2) Calculate the Number of the Newly Generated Clusters $N_{\text{NewNum}}\left(t\right)$

According to the non-stationary channel modeling procedure in [18], $N_{\text{NewNum}}\left(t\right)$ follows the Poisson distribution whose mean value and variance are both equal to

$$L = \text{E}\left\{N_{\text{NewNum}}\left(t\right)\right\} = \frac{\lambda_G}{\lambda_R}\left(1 - P_r\left(t\right)\right). \tag{41}$$

To generate a Poisson RV, we use the method of Ahrens and Dieter as described in [38], and derive the mean number of ROs for generating a Poisson RV is

$$C_{\text{NewNum}} = 7\left(L+1\right) \tag{42}$$

which is also the mean complexity to calculate the number of the newly generated clusters.

B. GENERATION OF NON-STATIONARY SSPS

1) Update Time-Variant Cluster Delays

For the newly generated clusters, the delays are calculated by using the same method as that in the initial channel response generation. Thus, similar to (10), the mean number of required ROs for generating delays for newly generated clusters is

$$C_{\text{NewDel}} = L^2 + 7L + 1. \tag{43}$$

According to (39) and (41), the mean number of the survived clusters is

$$\text{E}\{N_{\text{SurNum}}\left(t\right)\} = \text{E}\{N_{\text{total}}\left(t\right)\} - \text{E}\{N_{\text{NewNum}}\left(t\right)\} = N - L. \tag{44}$$

For each survived cluster, the time-varying delay $\tau_n\left(t_k\right)$ can be expressed as

$$\tau_n\left(t\right) = \frac{\left(c\left(t\right) - c\left(t_0\right)\right) + \left(a\left(t\right) - a\left(t_0\right)\right)}{c_0} + \tilde{\tau}_n\left(t_k\right). \tag{45}$$

Here, the distance between BS and the first bounce/scatterer, $c\left(t\right) = \sqrt{c^2\left(t_0\right) + \left(v_c t\right)^2 - 2c\left(t_0\right) v_c t \cos\left(\pi + \phi_{n,m}\left(t_0\right) - \theta_c\right)}$ and the distance between the last bounce/scatterer and MS, $a\left(t\right) = \sqrt{a^2\left(t_0\right) + \left(vt\right)^2 - 2a\left(t_0\right) vt \cos\left(\varphi_{n,m}\left(t_0\right) - \theta_v\right)}$ need to be calculated. Computation of each distance needs 2 real square operations, 5 real multiplications, 2 real subtractions, 1 real addition, and 1 cosine, totaling 18 ROs.

As shown in [18], the delay of the virtual link $\tilde{\tau}_n$ can be calculated using a first-order filtering algorithm as

$$\tilde{\tau}_n(t_k) = e^{(t_{k-1}-t_k)/\varepsilon}\tilde{\tau}_n(t_{k-1}) + \left(1 - e^{(t_{k-1}-t_k)/\varepsilon}\right) X \tag{46}$$

where $X \sim \mathrm{U}\left(\frac{D_{LoS}}{c_0}, \tau_{\max}\right)$. c_0 is the speed of light, D_{LoS} is the distance of the LoS path, $\tau_{\max}$ is the maximum delay, and ε is a parameter that depends on the coherence of a virtual link and scenario. 5 ROs are required to generate the uniform RV X, while 16 ROs are needed for the exponential part $e^{(t_{k-1}-t_k)/\varepsilon}$. Computing the right part of (46) requires 2 real multiplications, 1 real addition, and 1 subtraction. Thus, $5 + 16 + 4 = 25$ ROs are needed for generating $\tilde{\tau}_n(t_k)$.

Computing the delay of each survived cluster $\tau_n(t)$ needs 4 extra real additions and 1 real division in (45). Thus, the total number of ROs required is $18 \times 2 + 25 + 5 = 65$. As a result, updating the delays of all the survived clusters needs $C_{\mathrm{SurDel}} = 65(N - L)$ ROs in average.

2) Update Time-Variant Cluster Powers

Generating the powers of all the clusters follows the procedure of the original WSS IMT-A MIMO channel model and can be finished by replacing τ_n by $\tau_n(t)$ in (11). The mean number of clusters is still equal to N, so the mean number of ROs required is the same as that in (12).

3) Update Time-Variant Angular Parameters

The time-variant angular parameters of the newly generated clusters need to be generated by the same procedure in Section II. According to (17), the required number of ROs is

$$C_{\mathrm{NewAngGen}} = 173L + 4ML - 1. \tag{47}$$

After the angular parameter generation for the newly generated clusters, the random coupling from AoDs to AoAs can be realized with $C_{\mathrm{NewCoup}} = 5ML$ ROs. Thus, the number of ROs required for generating and coupling angular parameters for all newly generated clusters is

$$\begin{aligned} C_{\mathrm{NewAng}} &= C_{\mathrm{NewAngGen}} + C_{\mathrm{NewCoup}} \\ &= 173L + 9ML - 1. \end{aligned} \tag{48}$$

The AoDs and the AoAs of each survived cluster need to be regenerated according to the equations (26) and (33) in [18]. The arc-cosine operation can be finished by using a lookup table with the same number of ROs as the cosine function. Then, 39 ROs are needed for computing the AoD or AoA of one ray. The total number of ROs to generate the angular parameters for survived clusters is

$$C_{\mathrm{SurAng}} = 2{\times}39M(N - L) = 78M(N - L). \tag{49}$$

For the survived clusters, the coupling between AoDs and AoAs would not be updated.

C. GENERATION OF NON-STATIONARY CHANNEL COEFFICIENTS FOR MULTIPLE TIME SAMPLES

The time-variant channel coefficients of the non-stationary IMT-A MIMO channel model can be generated by substituting the time-varying channel parameters in (23). The random initial phases $\Phi_{n,m}(t)$ and FPs are still fixed, so C_Φ and C_{FP} can be ignored in the complexity analysis. For the non-stationary IMT-A MIMO channel model, in (23), only $\mathbf{A}_{n,m}$ is time-invariant while all other parameters need to be updated, i.e., 65 ROs can be ignored when ρ = 2 and 15 ROs can be reduced when ρ = 1 per ray per antenna pair. According to (29), the total complexity to regenerate the instantaneous channel coefficient is

$$C_{\mathrm{cc\_t}} = 119USNM - 2USN - 8US, \text{if } \rho = 2; \tag{50a}$$

$$C_{\mathrm{cc\_t}} = 89USNM - 2USN - 8US, \text{if } \rho = 1. \tag{50b}$$

Then, the total complexity per time sample to update all the time-variant parameters and to generate the channel coefficients of the non-stationary channel model can be expressed as

$$\begin{aligned} C_{\mathrm{NonSta\_t}} = (C_{\mathrm{NewNum}} + C_{\mathrm{SurNum}}) + (C_{\mathrm{NewDel}} + C_{\mathrm{SurDel}}) \\ + C_{\mathrm{P}} + (C_{\mathrm{NewAng}} + C_{\mathrm{SurAng}}) + C_{\mathrm{cc\_t}}. \end{aligned} \tag{51}$$

If T samples at temporal domain are generated and all parameters are updated for each sample, the total complexity of the non-stationary IMT-A MIMO channel model is

$$C_{\mathrm{NonSta}} = C_{\mathrm{initial}} + (T - 1)\, C_{\mathrm{NonSta\_t}}. \tag{52}$$

The computational complexities of different steps for the original WSS and non-stationary IMT-A MIMO channel models are summarized in Table 2.

IV. COMPLEXITY COMPARISON OF ORIGINAL WSS AND NON-STATIONARY IMT-A MIMO CHANNEL MODELS

Based on the analysis in Sections II and III, the complexities of the original WSS IMT-A MIMO channel model and the non-stationary IMT-A MIMO channel model will be compared. A rural macro (RMa) scenario is considered with the same parameter set as in [18], which is listed in Table 3. The speeds of the MS and mobile scatterer are 90 m/s and 30 m/s, respectively. The sampling interval was chosen as 1 transmission time interval (TTI), i.e., t_{sample} = 1 ms. For the convenience of comparing with measured data in [1], the central frequency was selected as 930 MHz.

The first two columns of Table 4 give the complexity comparison of these two models in the considered scenario. Numerical results of the ROs for different stages are listed. It can be observed that the processing related to channel coefficient matrix generation dominates the global complexity.

Fig. 1 shows the complexity comparison of the original WSS and non-stationary IMT-A MIMO channel models with different antenna pair numbers ($U \times S$). In total, 100 time samples are generated. The complexity increases linearly with the antenna pair number for both models. In Fig. 2, the complexity results are illustrated as a function of the time

TABLE 2. Computational complexities of the original WSS and non-stationary IMT-A MIMO channel models.

Stage	Step	The number of ROs	Values
Initial processing stage	LSP generation	C_{LS}	501
	Initial delay generation	C_{τ}	N^2+7N+1
	Initial power generation	C_{P}	$2N+109$
	Initial generations of AoAs and AoDs	C_{az}	$173N+4MN-1$
	Random coupling of rays within clusters	C_{coup}	$5MN$
	SSP generation	$C_{\text{SS}}=C_{\tau}+C_{\text{P}}+C_{\text{az}}+C_{\text{coup}}$	$N^2+182N+9MN+109$
	Random initial phases generation	C_{Φ}	$5\rho^2MN$
	Field pattern generation	C_{FP}	$9\left(U+S\right)\rho MN$
	Initial channel matrix generation	C_{H}	$\left(185M-2\right)USN-8US$, if $\rho=2$ $\left(104M-2\right)USN-8US$, if $\rho=1$
	Initial channel coefficients generation	C_{cc}	$C_{\Phi}+C_{\text{FP}}+C_{\text{H}}$
	Total generation for the initial sample	C_{initial}	$C_{\text{LS}}+C_{\text{SS}}+C_{\text{cc}}$
Generation of WSS IMT-A channel coefficients for multiple time samples	Channel coefficients matrix generation per sample for the WSS IMT-A MIMO model	$C_{\text{WSS\_t}}$	$36USNM-2USN-8US$
	Total complexity for the WSS IMT-A MIMO model	C_{WSS}	$C_{\text{initial}}+\left(T-1\right)C_{\text{WSS\_t}}$
Generation of non-stationary IMT-A channel coefficients for multiple time samples	Survived cluster number calculation	C_{SurNum}	$6N$
	Newly generated cluster number calculation	C_{NewNum}	$7(L+1)$
	Delay generation for survived clusters	C_{SurDel}	$65(N-L)$
	Delay generation for newly generated clusters	C_{NewDel}	L^2+7L+1
	Power generation	C_{P}	$2N+109$
	Angle generation for survived clusters	C_{SurAng}	$78M\left(N-L\right)$
	Angle generation for newly generated clusters	C_{NewAng}	$173L+9ML-1$
	Channel coefficients generation for the non-stationary IMT-A MIMO model	$C_{\text{cc\_t}}$	$119USNM-2USN-8US$, if $\rho=2$ $89USNM-2USN-8US$, if $\rho=1$
	Parameter update and channel coefficients matrix generation for the non-stationary IMT-A MIMO model	$C_{\text{NonSta\_t}}$	$(C_{\text{NewNum}}+C_{\text{SurNum}})+(C_{\text{NewDel}}+C_{\text{SurDel}})+C_{\text{P}}+(C_{\text{NewAng}}+C_{\text{SurAng}})+C_{\text{cc\_t}}$
	Total complexity of the non-stationary IMT-A MIMO model	C_{NonSta}	$C_{\text{initial}}+\left(T-1\right)C_{\text{NonSta\_t}}$

TABLE 3. Parameter setting for complexity analysis.

Parameters	Values
Mean cluster number (N)	10
Antenna configuration ($U\times S$)	2×2
Polarization (ρ)	1
Carrier frequency (f_c)	930 MHz
Generation rate of clusters (λ_G)	0.8/m
Recombination rate of new clusters (λ_R)	0.04/m
Percentage of moving clusters (P_c)	0.3
Speed of MS (v)	90 m/s
Speed of mobile scatterer (v_c)	30 m/s
Sampling interval (t_{sample})	1 ms

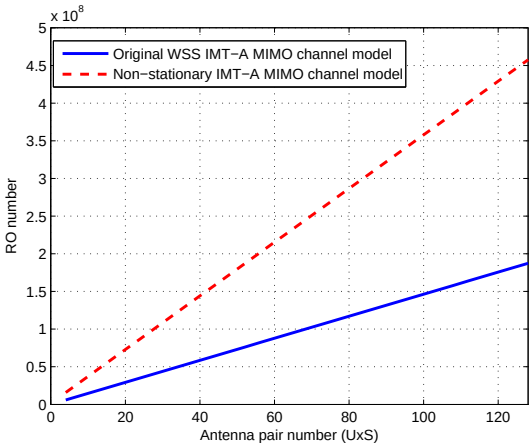

FIGURE 1. Complexity comparison of the original WSS and non-stationary IMT-A MIMO channel models with different antenna pair numbers in the considered HST scenario.

sample number T for the original WSS and non-stationary IMT-A MIMO channel models. With the increase of time samples, the required ROs increase linearly for both models. The intercepts of two curves (C_{initial}) are the same, while the slopes, corresponding to the ROs for generating channel coefficients per time sample, are different.

Fig. 3 shows the complexity comparison result of these two models, i.e., the ratio of the RO number of the non-stationary IMT-A MIMO channel model (C_{NonSta}) to that of the original WSS IMT-A MIMO channel model (C_{WSS}). When $T=1$, the same RO number is required to generate the initial sample in both models. With increasing T, the ratio becomes larger because the non-stationary IMT-A MIMO channel model needs more ROs to generate channel coefficients. When $T\rightarrow\infty$, the result tends to be the asymptotic value, i.e., $C_{\text{NonSta\_t}}/C_{\text{WSS\_t}}=3.05$ in this case.

In the meanwhile, we record the MATLAB channel coefficient computing time for generating channel coefficients with 10000 sets of 4×4 channel matrices. The parameter setting

TABLE 4. Example complexity comparison of the original WSS IMT-A MIMO channel model, the non-stationary IMT-A MIMO channel model, and the simplified non-stationary IMT-A MIMO channel models in the considered HST scenario.

Initial processing stage	**Original WSS IMT-A MIMO model**	**Non-Stationary IMT-A MIMO model**	**Non-stationary model without B-D process**	**Non-stationary model with fixed delays and powers**	**Non-stationary model with fixed AoDs**	**Non-stationary model with fixed AoDs and AoAs**
LSP generation (C_{LS})	501	501	501	501	501	501
SSP generation (C_{SS})	3829	3829	3829	3829	3829	3829
Random initial phases generation (C_{Φ})	1000	1000	1000	1000	1000	1000
Field pattern generation (C_{FP})	7200	7200	7200	7200	7200	7200
Initial channel coefficient matrix generation (C_{H})	91288	91288	91288	91288	91288	91288
Total generation for the initial sample ($C_{\mathbf{initial}}$)	**95618**	**95618**	**95618**	**95618**	**95618**	**95618**
Survived cluster number calculation (C_{SurNum})	0	60	0	0	0	0
Newly generated cluster number calculation (C_{NewNum})	0	7.2	0	0	0	0
Delay generation for survived clusters (C_{SurDel})	0	648.1	650	0	650	650
Delay generation for newly generated clusters (C_{SurDel})	0	1.2	0	0	0	0
Power generation (C_{P})	0	129	129	0	129	129
Angle generation for survived clusters (C_{SurAng})	0	15555	15600	15600	7800	0
Angle generation for newly generated clusters (C_{NewAng})	0	9.2	0	0	0	0
Channel coefficient matrix generation ($C_{\mathrm{WSS\_t}}$; $C_{\mathrm{cc\_t}}$)	28688	71088	71088	71088	67488	28688
RO per time sample	**28688**	**87498**	**87467**	**86688**	**76067**	**29467**
Complexity increase per time sample	**0%**	**205%**	**204.89%**	**202.18%**	**165.15%**	**2.72%**

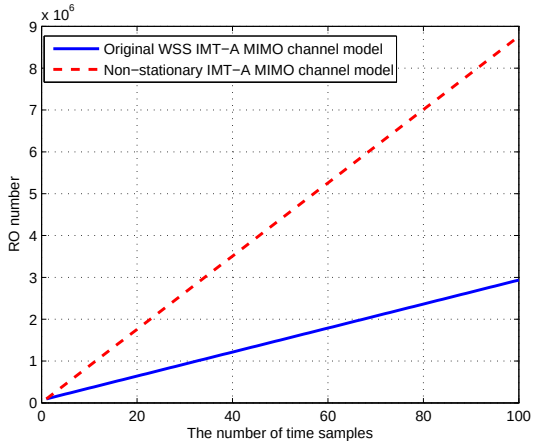

FIGURE 2. Complexity comparison of the original WSS and non-stationary IMT-A MIMO channel models with different time samples in the considered HST scenario.

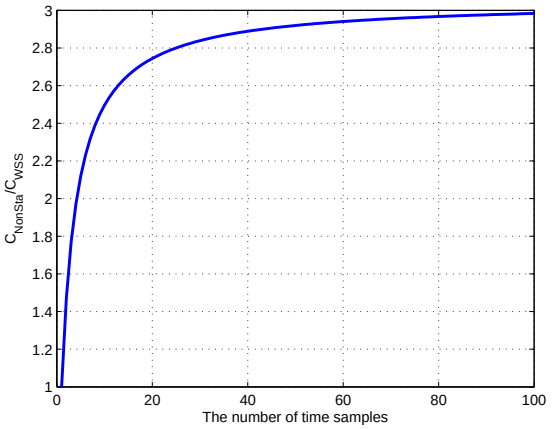

FIGURE 3. Complexity comparison between the original WSS and non-stationary IMT-A MIMO channel models with different time samples in the considered HST scenario.

is the same as that in Table 3. The PC we used to run the simulations has Intel Core i7, 4x2.93 GHz CPU, and 16 GB RAM. The computing times for the original WSS IMT-A MIMO channel model and the non-stationary IMT-A MIMO channel model are 0.3810 s and 1.1519 s, respectively. Correspondingly, the simulation time of the non-stationary IMT-A MIMO channel model is about 3.38 times of that of the original WSS IMT-A MIMO channel model.

According to the complexity analysis in terms of the required number of ROs and simulation time, it is shown that the computational complexity of the non-stationary IMT-A MIMO channel model is several times of that of the original WSS IMT-A MIMO channel. Even with the original IMT-A channel model, vast time consumption is needed for implementing the system-level simulations because multiple BSs and MSs and numerous drops are required. The introduction of non-stationarity will aggravate this problem. Thus, it is necessary to reduce the complexity of the proposed non-stationary IMT-A MIMO channel model without losing much accuracy for practical applications.

V. COMPLEXITY REDUCTION METHODS

In this section, two complexity reduction methods for the non-stationary IMT-A MIMO channel model are presented. The first method is to fix some channel parameters in the non-stationary channel models and the second one is to reduce the updated rate of all these time-variant parameters in the simulation. The purpose of these methods is to reduce the complexity while keeping the statistical properties as accurate as possible. The number of ROs is still used to analyze the computational complexity. For accuracy metrics, we consider several statistical properties including the spatial

CCF, temporal ACF, and stationary interval. The spatial CCF and temporal ACF are two important one-dimensional (1D) correlation functions, which are widely used in the evaluation and optimization of communication systems [32]. Stationary interval is used to measure the time interval in which the statistics of the channel do not change significantly.

A. FIXING SOME TIME-VARIANT CHANNEL PARAMETERS

In [27] and [28], parameters such as cluster number and delay spread in different drops were fixed for different drops to improve the computational efficiency of the GBSMs. In the non-stationary IMT-A MIMO channel model, all the time-variant parameters including the cluster number, powers, delays, AoDs, and AoAs need to be updated for each time sample t ($t = 0, \cdots, T-1$). In order to reduce the model complexity, some channel parameters can be viewed as static during the generation process of the non-stationary channel coefficients. We firstly analyze the impacts of these time-variant parameters on different statistic properties and then evaluate the complexity reduction and accuracy degradation resulted by fixing different channel parameters.

1) Statistical Properties

The spatial CCF can reflect the correlation property in the space domain. For WSS channels, CCF is only determined by the relative BS and MS antenna element spacings, i.e., $\Delta d_s = |d_{s_1} - d_{s_2}|$ and $\Delta d_u = |d_{u_1} - d_{u_2}|$. However, in the non-stationary IMT-A MIMO channel model, it depends on not only the relative antenna spacings, but also time t. The local spatial CCF of the n-th cluster can be expressed as [39], [40]

$$\begin{aligned}&\rho_{s_2u_2,n}^{s_1u_1}(t,\Delta d_s,\Delta d_u)\\&\quad=\mathrm{E}\left\{h_{u_1,s_1,n}(t)\,h_{u_2,s_2,n}^{*}(t)\right\}\\&\quad=\frac{1}{M}\sum_{m=1}^{M}\mathrm{E}\left\{P_n(t)\,e^{jk\Delta d_s\sin(\phi_{n,m}(t))}e^{jk\Delta d_u\sin(\varphi_{n,m}(t))}\right\}.\end{aligned}\tag{53}$$

According to equation (53), the local spatial CCF at time sample t is affected by the AoDs $\phi_{n,m}(t)$ and AoAs $\varphi_{n,m}(t)$.

The local temporal ACF of the n-th cluster can be expressed as [39], [40]

$$\begin{aligned}&r_n(t,\Delta t)=\mathrm{E}\left\{h_{u,s,n}(t)\,h_{u,s,n}^{*}(t-\Delta t)\right\}\\&=e^{-\lambda_R(v\Delta t+P_cv_c\Delta t)}\\&\times\frac{1}{M}\sum_{m=1}^{M}\mathrm{E}\left\{P_n(t)A_{\varphi_{n,m}}(t,\Delta t)B_{\phi_{n,m}}(t,\Delta t)C_{\varphi_{n,m}}(t,\Delta t)\right\}\end{aligned}\tag{54}$$

where

$$A_{\varphi_{n,m}}(t,\Delta t)=e^{j2\pi\lambda^{-1}d_u[\sin(\varphi_{n,m}(t))-\sin(\varphi_{n,m}(t+\Delta t))]},\tag{55a}$$

$$B_{\phi_{n,m}}(t,\Delta t)=e^{j2\pi\lambda^{-1}d_s[\sin(\phi_{n,m}(t))-\sin(\phi_{n,m}(t+\Delta t))]},\tag{55b}$$

$$\begin{aligned}C_{\varphi_{n,m}}(t,\Delta t)=&e^{-j2\pi\lambda^{-1}v\cos(\varphi_{n,m}(t)-\theta_v)(t)}\\&\times e^{j2\pi\lambda^{-1}v\cos(\varphi_{n,m}(t+\Delta t)-\theta_v)(t+\Delta t)}.\end{aligned}\tag{55c}$$

The local temporal ACF is affected by the AoDs $\phi_{n,m}(t)$, AoAs $\varphi_{n,m}(t)$, and two parameters related with the B-D process, P_c and λ_R.

The stationary interval can be calculated using averaged power delay profiles (APDPs) which is expressed as [1]

$$\overline{P_h}(t_k,\tau)=\frac{1}{N_{PDP}}\sum_{k}^{k+N_{PDP}-1}|h_{u,s}(t_k,\tau)|^2\tag{56}$$

where $h_{u,s}(t_k,\tau)=\sum_{n=1}^{N}h_{u,s,n}(t_k)\,\delta(\tau-\tau_n)$ and N_{PDP} is the number of power delay profiles to be averaged. The correlation coefficient between two APDPs can be calculated as

$$c(t_k,\Delta t)=\frac{\int\overline{P_h}(t_k,\tau)\,\overline{P_h}(t_k+\Delta t,\tau)\,\mathrm{d}\tau}{\max\{\int\overline{P_h}(t_k,\tau)^2\,\mathrm{d}\tau,\int\overline{P_h}(t_k+\Delta t,\tau)^2\,\mathrm{d}\tau\}}.\tag{57}$$

Then, the stationary interval can be given by

$$T_s(t_k)=\max\{\Delta t|_{c(t_k,\Delta t)\geq c_{\text{thresh}}}\}\tag{58}$$

where c_{thresh} is a given threshold of the correlation coefficient. From (56), (57), and (58), the stationary interval is related to the powers, delays, AoAs, and AoDs of the clusters.

2) Complexity Reduction Analysis

In the non-stationary IMT-A MIMO channel model, the B-D process is used to calculate the instantaneous number of clusters. With the parameters in Table 3, each cluster remains from a time sample to the following one with the probability $P_{remain} = 0.9986$, which can be calculated by (34). Then, according to (41), the mean number of newly generated clusters $L = 0.029$ in the selected scenario. It means the cluster number would change slowly even with high mobile speed, e.g., 90 m/s. Thus, we can neglect the B-D process and fix the number of clusters in the following analysis.

If the B-D process is not considered, the ROs for generating the cluster number can be neglected, and the number of ROs needed for generating channel coefficients per time sample is shown in Table 4. Neglecting the B-D process can reduce about 0.04% of the ROs per time sample compared with the non-stationary IMT-A MIMO channel model with all time-variant parameters.

In the original WSS IMT-A MIMO channel model, the powers of the clusters are determined by the delay values. Therefore, the powers will be time-invariant when the delays of the clusters are fixed. Table 4 also lists the number of ROs

for the non-stationary IMT-A MIMO channel model with fixed delays and powers of clusters. Only the generation of the time-variant angular parameters is preserved. It can be seen that fixing the delays and powers of the clusters can reduce 0.95% of the ROs per time sample for this example.

If there are no moving scatterers near the BS, the AoDs can be viewed as time-invariant. Then the ROs for regenerating time-variant angular parameters can be reduced by half. At the same time, the field pattern at the Tx side is fixed, and $9S\rho MN$ ROs can be removed from the channel coefficient generation. As a result, 13.56% of ROs can be reduced as illustrated in Table 4. The same complexity reduction can be obtained when the AoAs are time-invariant.

If AoDs and AoAs are both fixed, the ROs for generating time-variant angular parameters are no longer necessary. At the same time, the first row and second row of (23) are fixed, and the number of ROs for generating the non-stationary channel coefficients is the same as that of the original WSS IMT-A MIMO channel model. As illustrated in Table 4, 67% of the ROs can be reduced.

3) Accuracy Degradation Analysis

To judge the accuracy degradation brought by complexity reduction methods, the errors between the statistic properties of the non-stationary IMT-A MIMO channel model and that of the simplified non-stationary model are evaluated. Simulations are carried out with the parameter set of Table 3. Carrier frequency, speed of MS, and threshold of the correlation coefficient are selected according to the measurement setup in [1] and are listed as follows: f_c = 930 MHz, v = 90 m/s, and c_{thresh} = 0.8.

The measure of the errors between the spatial CCF of the non-stationary IMT-A MIMO channel model and that of the simplified model is the mean-square error (MSE) defined by [41], which can be express as (59)

$$E_{\text{CCF},n}(t) = \frac{1}{d_{u,\max}} \frac{1}{d_{s,\max}} \int_0^{d_{u,\max}} \int_0^{d_{s,\max}} \left[\rho^{s1,u1}_{s2,u2,n}(t, d_u, d_s) - \tilde{\rho}^{s1,u1}_{s2,u2,n}(t, d_u, d_s)\right]^2 d(d_u)\, d(d_s). \tag{59}$$

Here, $d_{u,\max}$ and $d_{s,\max}$ denote the appropriate distances over which the CCF is of interest at the receiver and transmitter side, respectively. Here, $\rho^{s1,u1}_{s2,u2}(t, d_u, d_s)$ is the spatial CCF of the n-th cluster in the non-stationary IMT-A MIMO channel model, and $\tilde{\rho}^{s1,u1}_{s2,u2}(t, d_u, d_s)$ is the approximate CCF of the n-th cluster in the simplified model. d_u and d_s are the antenna element spacings at the BS and MS, respectively.

If only the spatial CCF at the MS side is taken into account, the MSE can be rewritten as

$$E_{\text{CCF},n}(t) = \frac{1}{d_{u,\max}} \int_0^{d_{u,\max}} \left[\rho^{u1}_{u2,n}(t, d_u) - \tilde{\rho}^{u1}_{u2,n}(t, d_u)\right]^2 d(d_u). \tag{60}$$

In our following analysis, $d_{u,\max} = 10\lambda$.

TABLE 5. Accuracy degradation and complexity reduction of the proposed non-stationary IMT-A MIMO channel model by fixing different channel parameters.

Fixed parameters	Complexity reduction	MSE for CCF (t=1s)	MSE for ACF (t=1s)	MSE for CCDF of stationary interval
Cluster number	0.04%	None	6e-07	None
Delay and powers	0.95%	None	None	0.0003
AoDs and AoAs	67%	0.0002	0.0735	0.0124

Similarly, the measure of the error between the exact ACF and the ACF of the simplified non-stationary IMT-A MIMO channel model is the MSE defined by

$$E_{\text{ACF},n}(t) = \frac{1}{\Delta t_{\max}} \int_0^{\Delta t_{\max}} \left[r_n(t, \Delta t) - \tilde{r}_n(t, \Delta t)\right]^2 d(\Delta t) \tag{61}$$

where $\Delta t_{\max}$ denotes an appropriate time interval $[0, \Delta t_{\max}]$ over which the ACF is of interest. In our following analysis, the value $\Delta t_{\max} = 0.1$ s turns out to be suitable. In (61), $r_n(t, \Delta t)$ is the ACF of the n-th cluster in the non-stationary IMT-A MIMO channel model, while $\tilde{r}_n(t, \Delta t)$ is the ACF in the simplified non-stationary model.

Table 5 lists the MSEs of ACF and CCF ($n = 1$) with different fixed channel parameters. With regard to the speed of MS and mobile scatterers, the appearance and disappearance of the clusters do not happen very frequently in the environments. Generally, the survival time of the cluster is longer than the stationary interval, so neglecting the B-D process will only introduce very small errors to the considered statistical properties. Although fixing the angular parameters can reduce about 2/3 of the complexity, it will also bring large errors to the statistical properties.

Fig. 4 illustrates the empirical complementary cumulative distribution functions (CCDFs) of stationary intervals for the measured HST channel data and the original WSS IMT-A MIMO channel model. The measurement data reported in [1] are used for comparison. The results of the non-stationary IMT-A MIMO channel model with all time-variant parameters, only time-variant delays and powers, and only time-variant angular parameters are also shown. It can be observed that our non-stationary IMT-A MIMO channel model can provide better agreement with the measured data than the original WSS IMT-A MIMO channel model. Fig. 4 shows that the time-variant angular parameters have a greater impact on the stationary intervals compared with the time-variant delays and powers. It means that fixing angular parameters would result in larger stationary intervals than fixing delays and powers. The MSEs between different CCDF curves are also listed in Table 5.

Based on the numerical results, fixing the number, delays, and powers of the clusters can only reduce less than 1% of the ROs while bringing small errors to the statistical properties. At the same time, fixing angular parameters will severely degrade the accuracy of the non-stationary IMT-A channel model while reducing 67% of the complexity. Thus, one

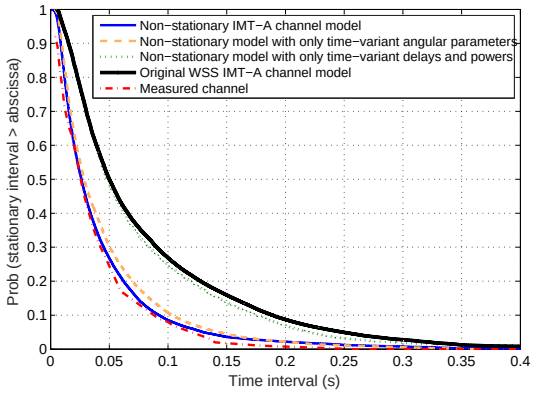

FIGURE 4. The empirical CCDFs of stationary intervals for the original WSS IMT-A MIMO channel model and the proposed non-stationary IMT-A MIMO channel model with all time-variant parameters, only time-variant delays and powers, and only time-variant angular parameters.

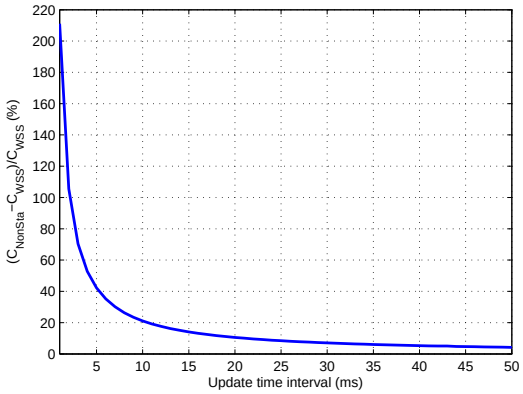

FIGURE 5. Complexity increase of the non-stationary IMT-A MIMO channel model with different update intervals compared with the original WSS IMT-A MIMO channel model.

should be very cautious to set the angular parameters time-invariant in the non-stationary IMT-A MIMO channel model. It is recommended that the selection of fixing parameters should be determined by the considered environment. For example, if the scatterers near the BS are static, then the AoDs of the clusters can be viewed as time-invariant. Moreover, the B-D process can be neglected if the environment changes slowly.

For comparison, the scheme proposed in [28] was also analyzed. In [28], the large-scale fading parameters are uncorrelated and fixed, which can reduce 501 ROs for generating the initial sample in comparison to our scheme. Besides, in [28], the cluster number and the delays are fixed which can reduce 846 ROs in comparison to our scheme that needs to generate time-variant parameters for each sample. As illustrated in Table 4, in total, 87498 ROs are required to update time-variant parameters and generate channel coefficients matrix per time sample for the non-stationary IMT-A MIMO model. Thus, only about 0.96% (846/87498) of ROs for each sample can be reduced with the scheme proposed in [28].

B. REDUCING THE UPDATE RATES OF TIME-VARIANT PARAMETERS

The previous analyses assume that the channel parameters need to be updated for every time sample in the non-stationary IMT-A MIMO channel model. However, as mentioned above, in realistic propagation environments the channel parameters satisfy the WSS condition over the stationary interval, which means that it is not necessary to update those parameters for each time sample. From Fig. 4, the measured stationary intervals are longer than 10 ms for 80% cases [1]. The update rate of channel parameters can be reduced in order to lower the computational complexity.

1) Complexity Reduction Analysis

Assume t_{sample} is the sampling interval between two consecutive time samples in the non-stationary IMT-A MIMO channel model. In general, the sampling interval is determined by the wavelength, the mobile speed, and the oversampling factor (number of time samples per half wavelength). As mentioned in Section IV, the sampling interval t_{sample} = 1 ms.

The update interval t_{update} is defined as the time interval for updating the time-variant parameters:

$$t_{\text{update}} = Qt_{\text{sample}} \tag{62}$$

which means that the time-variant channel parameters are updated every Q time samples. The channel parameters keep time-invariant within the update interval, and only the third row of (23) needs to be regenerated. Thus, the complexity for generating non-stationary channel coefficients are reduced to

$$C_{\text{NonSta}}(Q) = C_{\text{initial}} + \left\lfloor \frac{T-1}{Q} \right\rfloor C_{\text{NonSta\_t}} + \left(T - 1 - \left\lfloor \frac{T-1}{Q} \right\rfloor\right) C_{\text{WSS\_t}}. \tag{63}$$

Through increasing the update intervals, the complexity of the non-stationary IMT-A MIMO channel model can be effectively reduced. Fig. 5 compares the complexities of the non-stationary IMT-A MIMO channel models with different t_{update} values with that of the original WSS IMT-A MIMO channel model. The computational complexity increase is defined as

$$\text{CompInc}(t_{\text{update}}) = \frac{C_{\text{NonSta}}(t_{\text{update}}) - C_{\text{WSS}}}{C_{\text{WSS}}} \times 100\%. \tag{64}$$

For comparison, channel coefficients with 10000 sets of 2×2 channel matrices are generated, i.e., $T = 10000$. It is shown that if all the parameters are updated for each time sample, then the RO number of the non-stationary IMT-A MIMO channel model increases 211.16% compared with that of the original WSS IMT-A MIMO channel model as shown in Table 4. In Fig. 5, the complexity of the non-stationary IMT-A MIMO channel model increases 21.1% when $t_{\text{update}} = 10t_{\text{sample}}$. When $t_{\text{update}} \to \infty$, the non-stationary IMT-A MIMO channel model will degrade to the

TABLE 6. MSEs of statistic properties for the non-stationary IMT-A MIMO channel model with different update intervals.

Update interval (ms)	MSEs of CCFs ($\times 10^{-6}$)	MSEs of ACFs ($\times 10^{-6}$)
1	0	0
10	0.21	3.89
20	0.82	10.38
50	4.89	12.74
100	18.50	15.48

original WSS IMT-A MIMO channel model, i.e., all the channel parameters are time-invariant.

2) Accuracy degradation analysis

Reducing the update rate of time-variant parameters may affect the accuracy of the non-stationary IMT-A MIMO channel model. In Table 6, the MSEs of the spatial CCFs and temporal ACFs with different update intervals are listed. With increasing update intervals, it can be observed that the MSEs of channel statistical properties will also increase. If the update interval is chosen as 10 ms, the MSEs of the statistical properties are quite small. In this case, the computational complexity of the non-stationary IMT-A MIMO channel model only increases 21.1% compared with that of the original WSS IMT-A MIMO channel model. If we choose 50 ms as the update interval, the MSEs of spatial CCFs and temporal ACFs are larger but the RO number of the non-stationary IMT-A MIMO channel model only increases 4.2% compared with that of the original WSS IMT-A MIMO channel model.

Compared to the way of fixing the channel parameters, this method, i.e., reducing the update rates of time-variant parameters can efficiently reduce the complexity without losing much model accuracy. It should be noted that, when the update interval is too large, the MSEs of CCFs and ACFs will increase quickly. Thus, the update interval should be decided according to the stationary interval, and the tradeoff between the modeling complexity and accuracy requirements should be taken into account.

C. SIMPLIFICATION PROCEDURE FOR THE NON-STATIONARY IMT-A MIMO CHANNEL MODEL

The simplification procedure for the non-stationary IMT-A MIMO channel model can be carried out as follows.

(1) Choose the time-variant channel parameter set according to the simulation requirements.

(2) Extract the stationary interval values in a specified scenario from simulated or measured results.

(3) Determine the update interval of the time-variant channel parameters according to the stationary interval values.

(4) Compute the complexity of the simplified non-stationary IMT-A MIMO channel model and check if it satisfies the complexity requirement.

(5) Compute the channel statistical properties and check the accuracy requirement.

(6) Update the time-variant parameters according to the update interval and generate non-stationary channel coefficients for different time instances.

VI. CONCLUSIONS

In this paper, we have analyzed the complexities of the original WSS and the non-stationary IMT-A MIMO channel models in terms of the RO number and simulation time. The non-stationary IMT-A MIMO channel model can mimic the channel characteristics better in high-mobility scenarios, but at the cost of an extra computational complexity. Simulation results have demonstrated that the complexity of the non-stationary IMT-A MIMO channel model increases linearly with the increase of the numbers of generated time samples and antenna pairs, and is several times of that of the original WSS IMT-A MIMO channel model. To further improve the efficiency of the non-stationary IMT-A MIMO channel model, two complexity reduction methods have been proposed. The first method is to keep some channel parameters time-invariant when generating non-stationary channel coefficients. The accuracy degradation and complexity reduction of fixing different time-variant channel parameters have been compared. The second method is to increase the update interval of time-variant parameters. The update interval should be carefully chosen according to the stationary interval to ensure small errors of the produced channel statistical properties. Finally, the simplification procedure for the non-stationary IMT-A MIMO channel model has been provided.

REFERENCES

[1] B. Chen, Z. Zhong, and B. Ai, "Stationarity intervals of time-variant channel in high speed railway scenario," *J. China Commun.*, vol. 9, no. 8, pp. 64–70, Aug. 2012.

[2] A. Ispas, C. Schneider, G. Ascheid, and R. Thoma, "Analysis of the local quasi-stationarity of measured dual-polarized MIMO channels," *IEEE Trans. Veh. Technol.*, vol. 64, no. 8, pp. 3481–3493, Aug. 2015.

[3] J. Blumenstein *et al.*, "In-vehicle channel measurement, characterization, and spatial consistency comparison of 3–11 GHz and 55–65 GHz frequency bands," *IEEE Trans. Veh. Technol.*, vol. 66, no. 5, pp. 3526–3537, May 2017.

[4] K. Mahler, W. Keusgen, F. Tufvesson, T. Zemen, and G. Caire, "Measurement-based wideband analysis of dynamic multipath propagation in vehicular communication scenarios," *IEEE Trans. Veh. Technol.*, vol. 66, no. 6, pp. 4657–4667, June 2017.

[5] D. W. Matolak and R. Sun, "Air-ground channel characterization for unmanned aircraft systems-Part I: Methods, measurements, and models for over-water settings," *IEEE Trans. Veh. Technol.*, vol. 66, no. 1, pp. 26–44, Jan. 2017.

[6] Y. Liu, A. Ghazal, C.-X. Wang, X. Ge, Y. Yang, and Y. Zhang, "Channel measurements and models for high-speed train wireless communication systems in tunnel scenarios: A survey," *Sci. China Inf. Sci.*, vol. 60, no. 8, doi: 10.1007/s11432-016-9014-3, Oct. 2017.

[7] T. Zhou, C. Tao, L. Liu, H. Wen, and N. Zhang, "Analysis of time-frequency-space dispersion and nonstationarity in narrow-strip-shaped networks," in *Proc. IEEE WCNC*, Barcelona, Spain, 2018, pp. 1–6.

[8] C.-X. Wang, J. Bian, J. Sun, W. Zhang, and M. Zhang, "A survey of 5G channel measurements and models," *IEEE Commun. Surveys Tuts.*, vol. 20, no. 4, pp. 3142–3168, 4th Quart., 2018.

[9] Y. Liu, C.-X. Wang, and J. Huang, "Recent developments and future challenges in channel measurements and models for 5G and beyond high-speed train communication systems," *IEEE Commun. Mag.*, vol. 57, no. 9, pp. 50–56, Sept. 2019.

[10] J. Wu and P. Fan, "A survey on high mobility wireless communications: Challenges, opportunities and solutions," *IEEE Access*, vol. 4, no. 1, pp. 450–476, Jan. 2016.

[11] Y. Liu, C.-X. Wang, C. F. Lopez, and X. Ge, "3D non-stationary wideband circular tunnel channel models for high-speed train wireless communication systems," *Sci. China Inf. Sci.*, vol. 60, no. 8, doi: 10.1007/s11432-016-9004-4, Aug. 2017.

[12] J. Bian, J. Sun, C.-X. Wang, R. Feng, J. Huang, Y. Yang, and M. Zhang, "A WINNER+ based 3D non-stationary wideband MIMO channel model," *IEEE Trans. Wireless Commun.*, vol. 17, no. 3, pp. 1755–1767, Mar. 2018.

[13] S. Wu, C.-X. Wang, H. Aggoune, M. M. Alwakeel, and X. You, "A general 3D non-stationary 5G wireless channel model," *IEEE Trans. Commun.*, vol. 66, no. 7, pp. 3065–3078, July 2018.

[14] R. He, B. Ai, G. L. Stüber, and Z.-D. Zhong, "Mobility model-based non-stationary mobile-to-mobile channel modeling," *IEEE Trans. Wireless Commun.*, vol. 17, no. 7, pp. 4388–4400, Sept. 2018.

[15] Y. Liu, C.-X. Wang, J. Huang, J. Sun, and W. Zhang, "Novel 3D non-stationary mmWave massive MIMO channel models for 5G high-speed train wireless communications," *IEEE Trans. Veh. Technol.*, vol. 68, no. 3, pp. 2077–2086, Mar. 2019.

[16] Y. Liu, C.-X. Wang, C. F. Lopez, G. Goussetis, Y. Yang, and G. K. Karagiannidis, "3D non-stationary wideband tunnel channel models for 5G high-speed train wireless communications," *IEEE Trans. Intell. Transp. Syst.*, 2019, in press.

[17] J. Bian, C.-X. Wang, J. Huang, Y. Liu, J. Sun, M. Zhang, and H. Aggoune, "A 3D wideband non-stationary multi-mobility model for vehicle-to-vehicle MIMO channels," *IEEE Access*, vol. 7, no. 1, pp. 32562–32577, Mar. 2019.

[18] A. Ghazal, Y. Yuan, C.-X. Wang, Y. Zhang, H. Zhou, and W. Duan, "A non-stationary IMT-Advanced MIMO channel model for high-mobility wireless communication systems," *IEEE Trans. Wireless Commun.*, vol. 16, no. 4, pp. 2057–2068, Apr. 2017.

[19] P. Kyösti and T. Jämsä, "Complexity comparison of mimo channel modelling methods," in *Proc. IEEE ISWCS,* Trondheim, Norway, 2007, pp. 219–223.

[20] P. Kyösti, T. Jämsä, A. Byman, and M. Narandžić, "Computational complexity of drop based radio channel simulation," in *Proc. IEEE ISSSTA,* Bologna, Italy, 2008, pp. 287–291.

[21] J. Poikonen and J. Paavola, "Efficient channel models for network-level simulations," in *Proc. IEEE Chinacom,* Xi'an, China, 2009, pp. 1–6.

[22] A. F. Molisch, A. Kuchar, J. Laurila, K. Hugl, and E. Bonek, "Efficient implementation of a geometry-based directional model for mobile radio channels," in *Proc. IEEE VTC-Fall,* Amsterdam, Netherlands, 1999, pp. 1449–1453.

[23] B. Fleury, U. P. Bernhard, and R. Heddergott, "Advanced radio channel model for Magic WAND," in *Proc. ACTS Mobile Communications Summit,* Granada, Spain, 1996, pp. 600–607.

[24] F. Kaltenberger, T. Zemen, and C. W. Ueberhuber, "Low-complexity geometry-based MIMO channel simulation," *EURASIP J. Adv. Signal Process.*, vol. 2007, pp. 95281-1–95281-17, 2007.

[25] N. Czink, F. Kaltenberger, Y. Zhou, L. Bernad, T. Zemen, and X. Yin, "Low-complexity geometry-based modeling of diffuse scattering," in *Proc. EuCAP*, Barcelona, Spain, 2010, pp. 1–4.

[26] K.-W. Kim and S.-J. Oh, "An efficient implementation of the ITU-R channel model for device-to-device simulation," *IEEE Commun. Lett.,* vol. 18, no. 9, pp. 1633–1636, July 2014.

[27] Y. Zhang, J. Zhang, P. J. Smith, M. Shafi, and P. Zhang, "Reduced complexity channel models for IMT-Advanced evaluation," *EURASIP J. Wireless Commun. Networking,* vol. 2009, no. 1, pp. 1–13, Feb. 2009.

[28] X. Song, X. Ge, J. Zhang, and T. Han, "An improved IMT-A GBSM MIMO channel model," in *Proc. IEEE Globecom*, Austin, TX, USA, 2014, pp. 694–699.

[29] T. Fernández-Caramés, M. González-López, and L. Castedo, "FPGA-based vehicular channel emulator for real-time performance evaluation of IEEE 802.11p transceivers," *EURASIP J. Wireless Commun. Networking,* vol. 2010, no. 1, pp. 1–18, Apr. 2010.

[30] Z. Xu, M. Gan, and T. Zemen, "Cluster-based non-stationary vehicular channel model," in *Proc. EuCAP,* Davos, Switzerland, 2016, pp. 1–5.

[31] G. Ghiaasi *et al.,* "Real-time emulation of nonstationary channels in safety-relevant vehicular scenarios," *Wireless Commun. and Mobile Computing*, vol. 2018, pp. 1–18, May 2018.

[32] Q. Zhu *et al.,* "A novel 3D non-stationary wireless MIMO channel simulator and hardware emulator," *IEEE Trans. Commun.*, vol. 66, no. 8, pp. 3865–3878, Mar. 2018.

[33] M. Hofer *et al.,* "Validation of a real-time geometry-based stochastic channel model for vehicular scenarios," in *Proc. IEEE VTC-Spring*, Porto, Portugal, 2018, pp. 1–5.

[34] M. Hofer *et al.,* "Real-time geometry-based wireless channel emulation," *IEEE Trans. Veh. Technol.*, vol. 68, no. 2, pp. 1631–1645, Feb. 2019.

[35] "Guidelines for evaluation of radio interface technologies for IMT-advanced," Geneva, Switzerland. Tech. Rep. ITU-R M.2135-1, Dec. 2009.

[36] P. Kyösti *et al.*, WINNER II Channel Models Version 1.1, Sep. 2007, [Online]. Available: http://www.ist-winner.org/WINNER2-Deliverables/D1.1.2v1.1.pdf.

[37] T. Zwick, C. Fischer, D. Didascalou, and W. Wiesbeck, "A stochastic spatial channel model based on wave-propagation modeling," *IEEE J. Sel. Areas Commun.*, vol. 18, no. 1, pp. 6–15, Jan. 2000.

[38] D. E. Knuth, *The Art of Computer Programming,* vol. 2, Harlow, England: Addison-Wesley, 1969.

[39] Q. Yao, Y. Yuan, A. Ghazal, C.-X. Wang, L. Luan, and X. Lu, "Comparison of the statistical properties of the LTE-A and IMT-A channel models," in *Proc. IEEE WCNC*, Paris, France, 2012.

[40] Y. Liu, Y. Zhang, A. Ghazal, C. X. Wang, and Y. Yang, "Statistical properties of high-speed train wireless channels in different scenarios," in *Proc. IEEE VTC-Spring*, Nanjing, China, 2016, pp. 1–5.

[41] C.-X. Wang, D. Yuan, H.-H. Chen, and W. Xu, "An improved deterministic SoS channel simulator for efficient simulation of multiple uncorrelated Rayleigh fading channels," *IEEE Trans. Wireless Commun.,* vol. 7, no. 9, pp. 3307–3311, Sept. 2008.